PMU-based Estimation of Systematic Measurement Errors, Line Parameters and Tap Changer Ratios in Three-Phase Power Systems

Paolo Attilio Pegoraro, *Senior Member, IEEE*, Carlo Sitzia, *Student Member, IEEE*,
Antonio Vincenzo Solinas, *Graduate Student Member, IEEE*, Sara Sulis, *Senior Member, IEEE*

Abstract—The availability of accurate data is fundamental for several monitoring and control applications of modern power grids. Nevertheless, the knowledge of critical data such as transmission line and transformer parameters is often affected by uncertainty. This can lead to important problems in the correct management of the power systems. In spite of a monitoring infrastructure that is being renewed thanks to new generation devices providing synchronized measurements, the actual values of line parameters and tap changer ratios are still affected by uncertainty sources that need to be properly considered. The behaviour of all the elements involved in the measurement chain must be duly modelled. This paper proposes an improved method to carry out the simultaneous estimation of line parameters, tap changer ratios, and systematic measurement errors for a three-phase power system. The proposed method is based on the suitable modelling of the measurement chain and on three-phase constraint equations (voltage drop and current balance) of all the components involved. Its effectiveness is confirmed by tests performed on a IEEE 14 bus test system reproduced as a three-phase system under different operative conditions.

Index Terms—phasor measurement units, power transmission lines, tap changers, three-phase lines, measurement errors, step voltage regulators, instrument transformers, voltage measurements, current measurements.

I. Introduction

Accurate knowledge of power network parameters and actual operating conditions is essential for several monitoring and control applications. The transmission line parameters are critical for any application, but they are usually obtained from offline calculations based on assumptions concerning, for example, the conductors geometry and length, therefore actual values may be significantly different from those stored in the Transmission System Operator (TSO) database [1], [2]. The tap changer is critical, for example, in voltage stability applications [3], because the tap changer impacts on the margins of voltage stability and has important effects on voltage monitoring and control operations. The tap changer ratio is inevitably affected by uncertainty [4], furthermore, voltage regulators, often based on local measurements, can

P. A. Pegoraro, C. Sitzia, A. V. Solinas and S. Sulis are with the Department of Electrical and Electronic Engineering of the University of Cagliari, Cagliari, Italy (email: [paolo.pegoraro,carlo.sitzia,v.solinas,sara.sulis]@unica.it).

call for frequent changes, accelerating wear and tear. Although malfunctioning of the equipment involved in the tap changer is not frequent [5], the on-load tap changer is one of the most error-prone parts in the transformer because its elements can suffer from both electrical and mechanical stress [6], [7]. The uncertainty on tap changer performance impacts on fundamental analysis tools like state estimation (see, for instance, [8] and [9]).

Voltage regulation is a critical tool for any power system, because the increasing penetration of distributed resources affects every level of the grids and regulation of the medium voltage level is increasingly needed. Regulation can be obtained with different systems and equipment, in primary and secondary substations and also along the lines [10], [11]. Commonly, it is possible to find solutions with single-phase regulators along with a transformer without load tap changer or transformers with load tap changers. The choice is often driven by considerations about maintenance or procedures to be followed in case of failure.

Methodologies designed to increase the knowledge about power grid components are therefore more and more required. For example, in [12], an ac power standard, for high voltages and high currents, permitting the correction of the systematic errors of the components is presented. Several procedures have been presented for the estimation of the line parameters both in transmission and in distribution grids [1], [13]–[17], but none of these considers the impact of the entire measurement chain also addressing systematic error estimation, which is intended for compensation purposes, and voltage regulation uncertainty estimation.

In the context of transmission systems, several papers consider the tap changer estimation problem in equivalent single-phase power grids. Among them, it is possible to cite as an example [18], where a power system state estimator that includes tap positions and uses an iterative method for taking into account properly zero-injections is proposed, and [19], where the problem of the tap position identification is addressed. In [8], the state estimation model is designed by including the tap settings (voltage transformer turns ratios or phase-shift transformer angles) as additional state variables by means of a measurement model transformed to a conventional nodal frame formulation, introducing one fictitious bus and

one fictitious branch for each transformer.

Accurate knowledge of the value of tap changer parameters affects also the effectiveness of network parameters estimation tools. Considering a Supervisory Control and Data Acquisition (SCADA) system, in [20] it is proposed the simultaneous estimation of line and transformer parameters, exploiting the relationships between the estimated state and the parameters of interest to estimate linearly the single-phase values of impedance, transverse susceptance and tap ratio.

New estimation procedures are often based on Phasor Measurement Units (PMU), thanks to their everyday increasing availability. In [21] and [22], algorithms for estimating the parameters of lines and transformers using synchronized phasor measurements at both ends of a line are presented. In both cases, measurement errors are simulated by adding a noise to the results obtained from load flow solutions. In [23], a phasor-measurement-based state estimator for improving data consistency is proposed with features such as current channel scaling and estimation of tap position and line parameters, which can be achieved if a current phasor measurement is available and provided that sufficient measurement redundancy is ensured. In [24] a phasor-only state estimator is presented, allowing corrections for phase biases, transformer taps, and current magnitude scaling. The method is validated on a real system, therefore it is not possible to assess properly the impact of the uncertainty in the measurement chain on the estimates. In [13] a method for online identification of positive-sequence series transmission line and power transformer parameters is developed. The procedure is described as permitting also the estimation of negative- and zero-sequence parameters. However, also in this case, the measurement errors affecting the estimation results are taken into account applying only random noises to PMU data.

Another point to consider is that innovative proposals in this ambit are often validated under equivalent single-phase simplified operative conditions. Nevertheless, after this first validation stage, an extension to more realistic conditions is also required. The single-phase equivalent model can only provide the estimation of the parameters corresponding to the positive sequence, which are different from the parameters that should be evaluated in slightly unbalanced systems, as modern transmission grids actually are. Indeed, three-phase modeling allows the real parameters of physical systems to be estimated. Moreover, it is worth noticing that the estimation of the systematic errors introduced by ITs is directly related to a three-phase model because measurements are obtained on a per-phase basis: only a three-phase model would allow, for instance, to identify specific degradation of the metrological performance of a single IT or of the parameters in a given phase.

In the context of three-phase power grids, this paper addresses the simultaneous estimation of line parameters and tap changer ratios and the compensation of the systematic errors introduced by the measurement chain, which includes ITs affecting voltage and current synchronized phasor measurements. To the knowledge of the authors, in the literature this kind of estimation problem has not yet been addressed considering the whole measurement chain and its different uncertainty sources.

The procedure is performed considering some of the most used Step Voltage Regulator (SVR) configurations in three-phase systems and can be applied from the single branch to the entire network. The paper is based on the method proposed in [25], where the estimation problem was faced in the ambit of equivalent single-phase networks. Now a three-phase model of each component of the network is developed, focusing, in particular, on the proper modelling of three-phase SVR for wye and closed delta connections [26]. The problem is formulated considering also prior knowledge and is addressed in the Weighted Least Squares (WLS) sense. Validation tests, also using experimental PMU errors, are carried out considering both single-branch and multiple-branches approaches on a three-phase version of the IEEE 14-bus grid. The presented results prove that the proposed three-phase approach can be successfully applied with two of the most used SVR configurations, significantly improving the estimation accuracy in the presence of a realistic measurement chain.

The paper is organized as follows. In Section II, the adopted models and the proposed method are discussed. Section III method's performance is extensively assessed. Finally, Section IV provides some closing remarks and future research ideas.

II. PROPOSED METHOD

A. Transmission Line and Measurement Model

The three-phase line model shown in Fig. 1, corresponding to the generic branch (i, j) of a transmission line, is considered. The line model can be represented by means of two 3×3 matrices $\mathbf{Z}_{ij}$ and $\mathbf{Y}_{\text{sh},ij}$, i.e. the impedance matrix and shunt admittance matrix, respectively, that can be written as:
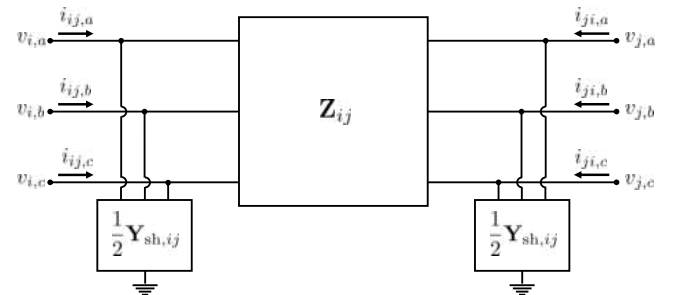
Fig. 1. Three-phase scheme for a transmission network branch and available measurements.

$$\mathbf{Z}_{ij} = \begin{bmatrix} z_{ij,aa} & z_{ij,ab} & z_{ij,ac} \\ z_{ij,ab} & z_{ij,bb} & z_{ij,bc} \\ z_{ij,ac} & z_{ij,bc} & z_{ij,cc} \end{bmatrix} \quad (1)$$

$$\mathbf{Y}_{\text{sh},ij} = \begin{bmatrix} y_{\text{sh},ij,aa} & y_{\text{sh},ij,ab} & y_{\text{sh},ij,ac} \\ y_{\text{sh},ij,ab} & y_{\text{sh},ij,bb} & y_{\text{sh},ij,bc} \\ y_{\text{sh},ij,ac} & y_{\text{sh},ij,bc} & y_{\text{sh},ij,cc} \end{bmatrix} \quad (2)$$

In the entries of both matrices, the subscripts ij indicate the end nodes of the (i, j) branch, while the subscripts pq

with $p, q \in \{a, b, c\}$ indicate the corresponding phases pair. Thus $z_{ij,pq}$ is the line impedance (or the mutual impedance when $p \neq q$) and $b_{\text{sh},ij,pq}$ is the shunt admittance between phase p and q. The shunt admittance is assumed to be equally divided into the two sides of the three-phase π-line model of each branch, and it is assumed to be a pure susceptance, thus giving $y_{\text{sh},ij,pq} = jB_{\text{sh},ij,pq}$ and $\mathbf{Y}_{\text{sh},ij} = j\mathbf{B}_{\text{sh},ij}$.

In this paper, the availability of PMUs installed on both sides of each branch is assumed. The synchronized measurements provided by the PMUs are the 3 phase voltage synchrophasor measurements $v_{h,p}$, with $p = \{a, b, c\}$, for each node $h \in \{i, j\}$, that is at the start and end nodes. The 6 current synchrophasor measurements $i_{ij,p}$ and $i_{ji,p}$ are also measured. The synchronized measurements can be time-aligned (labelled with an UTC timestamp t) and thus represent a coordinated set of measurements referred to the same time instant t.

The line model defines a measurement model that links the set of measured values to the line parameters, which are not perfectly known, and to the errors that affect every measured value. Each measured synchrophasor can be expressed as a function of reference values (indicated in the following equations by superscript ^{R}) and of measurement errors as follows:

$$
\begin{aligned}
v_{h,p} &= V_{h,p}e^{j\varphi_{h,p}} = V_{h,p}^r + jV_{h,p}^x \\
&= (1 + \xi_{h,p}^{sys} + \xi_{h,p}^{rnd})V_{h,p}^R e^{j(\varphi_{h,p}^R + \alpha_{h,p}^{sys} + \alpha_{h,p}^{rnd})} \\
i_{ij,p} &= I_{ij,p}e^{j\theta_{ij,p}} = I_{h,p}^r + jI_{h,p}^x \\
&= (1 + \eta_{ij,p}^{sys} + \eta_{ij,p}^{rnd})I_{ij,p}^R e^{j(\theta_{ij,p}^R + \psi_{ij,p}^{sys} + \psi_{ij,p}^{rnd})}
\end{aligned}
\tag{3}
$$

where $V_{h,p}$ and $\varphi_{h,p}$ are the magnitude and phase-angle measurements of node h voltage at phase p. Analogously, $I_{ij,p}$ and $\theta_{ij,p}$ are the measured magnitude and phase angle of the p-phase branch current flowing from node i towards node j. Measured current phasor $i_{ji,p}$ (see Fig. 1) can be expressed in a similar way. Superscripts ^{r} and ^{x} are used for the real and imaginary parts of the corresponding phasors. Finally, superscripts ^{sys} and ^{rnd} refer to the systematic and random errors, respectively. The main difference between these errors is that systematic errors are the same across repeated measurements, while random errors vary from one observation to another. To model the uncertainty contributions, in the following, the systematic measurement errors are attributed mainly to ITs and the random errors to PMUs. The errors, as indicated in (3), affect both magnitudes and phase angles of each synchrophasor measurements. In particular, quantities $\xi_{h,p}^{sys}$ and $\eta_{ij,p}^{sys}$ (or $\eta_{ji,p}^{sys}$) refer to the systematic ratio errors of the voltage and current phasors at node h and phase p, respectively. Moreover, $\alpha_{h,p}^{sys}$ and $\psi_{ij,p}^{sys}$ (or $\psi_{ji,p}^{sys}$) are the systematic phase displacement errors for the above defined measurements. These quantities can be assumed as the unknowns in the measurement model. Analogously, replacing ^{sys} with ^{rnd}, the corresponding random ratio and phase displacement errors can be defined.

It is realistic to assume that all the absolute values of these errors are much lower than one (i.e. $|err| \ll 1$, with $err \in$ $\{\xi, \alpha, \eta, \psi\}$), as in [25], and thus it is possible, adopting a first order approximation, to rewrite (3) to express each reference synchrophasor as function of the measured values and of the above defined errors (h and p have same meaning as before):

$$
\begin{aligned}
v_{h,p}^R &\simeq \left(V_{h,p}^r + jV_{h,p}^x\right)\left(1 - \xi_{h,p}^{sys} - \xi_{h,p}^{rnd} - j\alpha_{h,p}^{sys} - j\alpha_{h,p}^{rnd}\right) \\
i_{ij,p}^R &\simeq \left(I_{ij,p}^r + jI_{ij,p}^x\right)\left(1 - \eta_{ij,p}^{sys} - \eta_{ij,p}^{rnd} - j\psi_{ij,p}^{sys} - j\psi_{ij,p}^{rnd}\right)
\end{aligned}
\tag{4}
$$

Current phasor $i_{ji,p}^R$ can be similarly defined.

Considering (1) and (2), it is possible to rewrite the generic line parameter, that is the generic element (p, q) in the matrices $\mathbf{Z}_{ij}$ and $\mathbf{B}_{\text{sh},ij}$, as:

$$
\begin{aligned}
z_{ij,pq} &= R_{ij,pq} + jX_{ij,pq} \\
&= R_{ij,pq}^0(1 + \gamma_{ij,pq}) + jX_{ij,pq}^0(1 + \beta_{ij,pq}) \\
B_{\text{sh},ij,pq} &= B_{\text{sh},ij,pq}^0(1 + \rho_{ij,pq})
\end{aligned}
\tag{5}
$$

where $\gamma_{ij,pq}$, $\beta_{ij,pq}$ and $\rho_{ij,pq}$ (p and $q \in \{a, b, c\}$) are the relative deviations of resistance, reactance and transversal susceptance values, respectively, from $R_{ij,pq}^0$, $X_{ij,pq}^0$ and $B_{\text{sh},ij,pq}^0$ available in TSO database (superscript ^{0} indicates nominal values).

As in [25], the procedure aims at estimating all the systematic measurement errors and all the parameters' deviations. The estimation algorithm can thus rely on the constraints given by Kirchhoff's laws, which correspond to the following three-phase line voltage drop constraints and three-phase current balance equations:

$$
\left(\mathbf{v}_i^R - \mathbf{v}_j^R\right) = \mathbf{Z}_{ij}\left(\mathbf{i}_{ij}^R - j\frac{\mathbf{B}_{\text{sh},ij}}{2}\mathbf{v}_i^R\right)
\tag{6}
$$

$$
\left(\mathbf{i}_{ij}^R + \mathbf{i}_{ji}^R\right) = j\frac{\mathbf{B}_{\text{sh},ij}}{2}\left(\mathbf{v}_i^R + \mathbf{v}_j^R\right)
\tag{7}
$$

where $\mathbf{v}_h^R = \left[v_{h,a}^R \; v_{h,b}^R \; v_{h,c}^R\right]^{\mathsf{T}}$ is the voltage phasors vector of the h node, while $\mathbf{i}_{ij}^R = \left[i_{ij_a}^R \; i_{ij_b}^R \; i_{ij_c}^R\right]^{\mathsf{T}}$ and $\mathbf{i}_{ji}^R = \left[i_{ji_a}^R \; i_{ji_b}^R \; i_{ji_c}^R\right]^{\mathsf{T}}$ are the three-phase branch-current phasor vectors leaving nodes i and j, respectively[1]. The Kirkhhoff's laws link reference phasors with actual line parameters. Then, by substituting the expressions (4) of reference phasors as function of measured values and errors and the actual line parameters from (5) into (6) and (7), it is possible to write a system of complex equations involving measurements and measurement errors. Applying a first order approximation as in [25] and finally splitting each complex equation into its real and imaginary part, a system of 12 real-valued linear equations can be obtained from the constraints. For these equations, the systematic errors and the parameter deviations can be considered as the unknowns, while random errors represent the model errors.

---

[1] T is the transpose operator.

B. Step Voltage Regulator and Measurement Model

In this paper, the three-phase SVR is modelled aiming at the simultaneous estimation of line parameters, systematic measurement errors and tap-changer ratios. More specifically, a comprehensive formulation of wye and closed delta connections is developed, showing the proposed method for both configurations (see, for example, [27] for details about these connections). The SVR is a device installed along the feeder or at the substation to keep the voltages within acceptable limits. It is a connection of an auto-transformer with a variable turn ratio [28], which is dependent on the position of the tap and is determined through a control circuit that uses the approximate voltage drop to command the displacement of the tap.

In this paper, the SVR is modelled as installed in a generic branch (l, k) with the same assumptions made for the transmission line branch. PMUs are available at both ends of the branch, providing the synchrophasor measurements $v_{h,p}$, $i_{lk,p}$ and $i_{kl,p}$ (with $h \in \{l, k\}$ and $p \in \{a, b, c\}$). The corresponding reference synchrophasors are indicated by $v_{h,p}^R$, $i_{lk,p}^R$ and $i_{kl,p}^R$, respectively. In the following, the pair of symbols (l, k) will be used to distinguish a branch with SVR from a generic line branch (i, j). Thus, (3) and (4) are still valid models for measured and reference synchrophasors of the SVR branch when $h \in (l, k)$ and ij is replaced with lk.

The relationship between voltage and current phasors at the primary and secondary of the SVR associated with branch (l, k) are obtained by means of the matrices $\mathbf{A}_{v,lk}$, $\mathbf{A}_{i,lk}$ and $\mathbf{Z}_{SVR,lk}$, which are the voltage gain, the current gain and the impedance matrix of the SVR, respectively [26]. For all the SVR connection typologies, the following relationship among the matrices $\mathbf{A}_{v,lk}$ and $\mathbf{A}_{i,lk}$ holds true:

$$\mathbf{A}_{v,lk}^{-1} = \mathbf{A}_{i,lk}^\mathsf{T} \tag{8}$$

The entries of the above-mentioned matrices are determined by the specific connection configuration, e.g. wye or closed delta. The models adopted by the proposed algorithm for these connections are presented in detail in the following.

For a wye-connected SVR the voltage gain matrix has the following structure:

$$\mathbf{A}_{v,lk} = \begin{bmatrix} a_{lk,aa} & 0 & 0 \\ 0 & a_{lk,bb} & 0 \\ 0 & 0 & a_{lk,cc} \end{bmatrix} \tag{9}$$

while, for a closed delta connected SVR the matrix is:

$$\mathbf{A}_{v,lk} = \begin{bmatrix} a_{lk,ab} & 1 - a_{lk,ab} & 0 \\ 0 & a_{lk,bc} & 1 - a_{lk,bc} \\ 1 - a_{lk,ac} & 0 & a_{lk,ac} \end{bmatrix} \tag{10}$$

The following expression is used to define the nonzero entries of $\mathbf{A}_{v,lk}$ for both wye and closed delta configurations:

$$a_{lk,pq} = a_{lk,pq}^0 \left(1 + \tau_{lk,pq}\right) \tag{11}$$

where $p, q \in \{a, b, c\}$ (the permitted combinations depend on the connection type), $a_{lk,pq}^0$ is the nominal or assumed value of the tap changer ratio, and $\tau_{lk,pq}$ is the relative deviation of

actual value from nominal one. In the following, tap changer ratio variations are assumed to be occurring with a longer timescale than PMU reporting rates, therefore $\tau_{lk,pq}$ can be considered as an additional unknown of the estimation process.

The impedance matrix $\mathbf{Z}_{SVR,lk}$ is considered diagonal and, similarly to the first equation in (5), its entries can be expressed as a function of the corresponding reactance value available from the TSO database and of the relative deviation from it. In particular, following the notation in [26], for wye connection $z_{lk,pp}$ is:

$$z_{lk,pp} = jX_{lk,pp}^0 \left(1 + \beta_{lk,pp}\right) \tag{12}$$

with $p \in \{a, b, c\}$. For closed delta configuration, the diagonal nonzero parameters are $z_{lk,ab}$, $z_{lk,bc}$ and $z_{lk,ac}$ and depend on the associated $\beta_{lk,ab}$, $\beta_{lk,bc}$ and $\beta_{lk,ac}$ variables and on the corresponding reactances.

With the node admittance matrix $\mathbf{Y}_{lk}$ of branch (l, k), and considering the three-phase model of the SVR, it is possible to define the following constraints:

$$\begin{bmatrix} \mathbf{i}_{lk}^R \\ \mathbf{i}_{kl}^R \end{bmatrix} = \mathbf{Y}_{lk} \begin{bmatrix} \mathbf{v}_l^R \\ \mathbf{v}_k^R \end{bmatrix} \tag{13}$$

where, analogously to the symbols used in Section II-A, $\mathbf{v}_h^R = \left[v_{h,a}^R \ v_{h,b}^R \ v_{h,c}^R\right]^\mathsf{T}$ is the vector of reference voltage phasors at node h ($h \in \{l, k\}$), while $\mathbf{i}_{lk}^R = \left[i_{lk,a}^R \ i_{lk,b}^R \ i_{lk,c}^R\right]^\mathsf{T}$ and $\mathbf{i}_{kl}^R = \left[i_{kl,a}^R \ i_{kl,b}^R \ i_{kl,c}^R\right]^\mathsf{T}$ are the reference branch-current phasor vectors departing from node l and k, respectively. $\mathbf{Y}_{lk}$ is the 6×6 matrix defined by:

$$\mathbf{Y}_{lk} = \begin{bmatrix} \mathbf{A}_{i,lk}\mathbf{Z}_{SVR,lk}^{-1}\mathbf{A}_{i,lk}^\mathsf{T} & -\mathbf{A}_{i,lk}\mathbf{Z}_{SVR,lk}^{-1} \\ -\mathbf{Z}_{SVR,lk}^{-1}\mathbf{A}_{i,lk}^\mathsf{T} & \mathbf{Z}_{SVR,lk}^{-1} \end{bmatrix} \tag{14}$$

Equation (13) and (14) can be used to define the constraints deriving by Kirchhoff's laws for the case of SVR. Choosing the SVR configuration and the corresponding matrix $\mathbf{A}_{v,lk}$ from (9) or (10). Exploiting also the relationship (8) and making explicit the voltages with respect to the currents, the voltage drop equations and the current balance equations associated with the SVR can be obtained as follows:

$$\mathbf{v}_l^R - \mathbf{A}_{v,lk}\mathbf{v}_k^R = \mathbf{A}_{v,lk}\mathbf{Z}_{SVR,lk}\mathbf{A}_{v,lk}^\mathsf{T}\mathbf{i}_{lk}^R \tag{15}$$

$$\mathbf{i}_{kl}^R = -\mathbf{A}_{v,lk}^\mathsf{T}\mathbf{i}_{lk}^R \tag{16}$$

With the same assumptions on the errors adopted in Section II-A, (15) and (16) can be written with a first order approximation, thus defining 6 complex-valued equations and thus a system of 12 real-valued equations for each SVR in the network. Such equations are reported in detail in the Appendix and link the measurements to all the unknown parameters to be estimated, including tap changer ratios.

C. Estimation Method for a Single Branch

The systems of linear equations described in Section II-A for the generic line (i, j) and in Section II-B for the SVR branch (l, k) are referred to a given set of synchronized measurements associated with a specific time instant t (the

timestamp of PMU measurements). It is thus possible to rewrite the system associated with a single branch with a matrix notation, separating the random errors from the systematic ones. Focusing only on the SVR case for the sake of brevity (similar expressions are valid also for a transmission line, which are the generalization of those reported in [25]), the following expression can be written:

$$\mathbf{b}_{lk,t} = \mathbf{H}_{lk,t} \begin{bmatrix} \boldsymbol{\xi}_l^{sys} \\ \boldsymbol{\alpha}_l^{sys} \\ \boldsymbol{\xi}_k^{sys} \\ \boldsymbol{\alpha}_k^{sys} \\ \boldsymbol{\eta}_{lk}^{sys} \\ \boldsymbol{\psi}_{lk}^{sys} \\ \boldsymbol{\eta}_{kl}^{sys} \\ \boldsymbol{\psi}_{kl}^{sys} \\ \boldsymbol{\beta}_{lk} \\ \boldsymbol{\tau}_{lk} \end{bmatrix} + \mathbf{E}_{lk,t} \begin{bmatrix} \boldsymbol{\xi}_{l,t}^{rnd} \\ \boldsymbol{\alpha}_{l,t}^{rnd} \\ \boldsymbol{\xi}_{k,t}^{rnd} \\ \boldsymbol{\alpha}_{k,t}^{rnd} \\ \boldsymbol{\eta}_{lk,t}^{rnd} \\ \boldsymbol{\psi}_{lk,t}^{rnd} \\ \boldsymbol{\eta}_{kl,t}^{rnd} \\ \boldsymbol{\psi}_{kl,t}^{rnd} \end{bmatrix} \quad (17)$$

$$= \mathbf{H}_{lk,t}\mathbf{x}_{lk} + \mathbf{E}_{lk,t}\mathbf{e}_{lk,t} = \mathbf{H}_{lk,t}\mathbf{x}_{lk} + \boldsymbol{\epsilon}_{lk,t}$$

where subscript t denotes the timestamp, $\mathbf{b}_{lk,t}$ is the vector of all known terms associated with the equations for branch (l,k) (the left side values in the equations of the Appendix) and $\mathbf{H}_{lk,t}$ is the matrix that gives the linear relationship between the equivalent measurements in $\mathbf{b}_{lk,t}$ and the vector of systematic errors and deviations. Vector $\mathbf{x}_{lk}$ includes all the unknowns of branch (l,k). As an example, it includes $\boldsymbol{\xi}_h^{sys} = \begin{bmatrix} \xi_{h,a}^{sys} & \xi_{h,b}^{sys} & \xi_{h,c}^{sys} \end{bmatrix}^\mathsf{T}$ ($h \in \{l,k\}$) that is the 3×1 vector including the systematic ratio errors for measured voltage synchrophasors at node h. Similar definitions hold for $\boldsymbol{\alpha}_h^{sys}$, $\boldsymbol{\eta}_{lk}^{sys}$, $\boldsymbol{\psi}_{lk}^{sys}$, $\boldsymbol{\eta}_{kl}^{sys}$, $\boldsymbol{\psi}_{kl}^{sys}$, $\boldsymbol{\beta}_{lk}$ and $\boldsymbol{\tau}_{lk}$. In particular, $\boldsymbol{\beta}_{lk} = [\beta_{lk,aa} \ \beta_{lk,bb} \ \beta_{lk,cc}]^\mathsf{T}$ and $\boldsymbol{\tau}_{lk} = [\tau_{lk,aa} \ \tau_{lk,bb} \ \tau_{lk,cc}]^\mathsf{T}$ for wye configuration, whereas $\boldsymbol{\beta}_{lk} = [\beta_{lk,ab} \ \beta_{lk,bc} \ \beta_{lk,ac}]^\mathsf{T}$ $\boldsymbol{\tau}_{lk} = [\tau_{lk,ab} \ \tau_{lk,bc} \ \tau_{lk,ac}]^\mathsf{T}$ for closed delta configuration.

Replacing ^{sys} with ^{rnd}, similar vectors can be defined also for random errors and they are grouped in $\mathbf{e}_{lk,t}$. Matrix $\mathbf{E}_{lk,t}$ transforms the measurement random errors in $\mathbf{e}_{lk,t}$ into the random error vector $\boldsymbol{\epsilon}_{lk,t}$ associated with the equivalent measurements in $\mathbf{b}_{lk,t}$.

When considering instead the system for the transmission line of branch (i,j), a vector of unknowns $\mathbf{x}_{ij}$ can be defined, which includes systematic errors for voltages and currents and deviations $\gamma_{ij,pq}$, $\beta_{ij,pq}$ and $\rho_{ij,pq}$, depending on the parameters present in the model. Analogously to the SVR case, matrices $\mathbf{H}_{ij,t}$, $\mathbf{E}_{ij,t}$ and vectors $\mathbf{e}_{ij,t}$ and $\boldsymbol{\epsilon}_{ij,t}$ can be used to define the corresponding system.

To estimate $\mathbf{x}_{lk}$, similarly to [25], multiple time instants $t_1, \cdots, t_{N_t}$ (and their corresponding three-phase measurement sets) are used altogether to define a multi-timestamp system as follows:

$$\mathbf{b}_{lk} = \begin{bmatrix} \mathbf{b}_{lk,t_1} \\ \vdots \\ \mathbf{b}_{lk,t_{N_t}} \end{bmatrix} = \begin{bmatrix} \mathbf{H}_{lk,t_1} \\ \vdots \\ \mathbf{H}_{lk,t_{N_t}} \end{bmatrix} \mathbf{x}_{lk} + \begin{bmatrix} \mathbf{E}_{lk,t_1} & & \mathbf{0} \\ & \ddots & \\ \mathbf{0} & & \mathbf{E}_{lk,t_{N_t}} \end{bmatrix} \begin{bmatrix} \mathbf{e}_{lk,t_1} \\ \vdots \\ \mathbf{e}_{lk,t_{N_t}} \end{bmatrix}$$

$$= \mathbf{H}_{lk}\mathbf{x}_{lk} + \mathbf{E}_{lk}\mathbf{e}_{lk} = \mathbf{H}_{lk}\mathbf{x}_{lk} + \boldsymbol{\epsilon}_{lk} \quad (18)$$

where $\mathbf{x}_{lk}$ is the same across different time instants and $\mathbf{E}_{lk}$ is block diagonal because the random errors of equivalent measurements at each instant t depend only on the random errors at the same instant.

Like in [25] and [29], without loss of generality, multiple PMU measurements are assumed to be available for each load condition and different load conditions (cases) are taken into account. Measurements obtained within a small time interval (repeated measurements for the same case) can be averaged and used to define a problem like (17) that represents a specific case. On this basis, the problem (18) can be considered as composed only of different cases, thus limiting the size of the system. If some measurements or timestamps are missing, it is easy to adapt the method according to available data.

In addition to the above mentioned equations, every source of prior information about the unknowns is also used and thus it is possible to rewrite the problem as:

$$\mathbf{b}_{lk,+} = \begin{bmatrix} \mathbf{b}_{lk} \\ \mathbf{0}_{r\times 1} \end{bmatrix} = \begin{bmatrix} \mathbf{H}_{lk} \\ \mathbf{I}_r \end{bmatrix} \mathbf{x}_{lk} + \begin{bmatrix} \boldsymbol{\epsilon}_{lk} \\ \mathbf{e}_{prior} \end{bmatrix} \quad (19)$$

$$= \mathbf{H}_{lk,+}\mathbf{x}_{lk} + \boldsymbol{\epsilon}_{lk,+}$$

where $\mathbf{0}_{r\times 1}$ is a r-size vector of zeros (r is the number of unknowns in $\mathbf{x}_{lk}$, which depends on the exact model and on the SVR connection type) that defines the pseudo-measurements associated with prior information (i.e. no deviations is assumed) and $\mathbf{I}_r$ is the identity matrix of size r, representing the measurement matrix of prior values. Vector $\boldsymbol{\epsilon}_{lk,+}$ includes both the equivalent random errors $\boldsymbol{\epsilon}_{lk}$ and the random variables $\mathbf{e}_{prior}$ associated with prior errors.

The problem (19) can be solved via WLS estimation, where the weight matrix $\mathbf{W}_{lk,+} = \boldsymbol{\Sigma}_{\boldsymbol{\epsilon}_{lk,+}}^{-1}$ with:

$$\boldsymbol{\Sigma}_{\boldsymbol{\epsilon}_{lk,+}} = \begin{bmatrix} \boldsymbol{\Sigma}_{\boldsymbol{\epsilon}_{lk}} & \mathbf{0} \\ \mathbf{0} & \boldsymbol{\Sigma}_{\mathbf{e}_{prior}} \end{bmatrix} \quad (20)$$

the covariance matrix of equivalent measurements and priors. The covariance matrix of $\boldsymbol{\epsilon}_{lk}$ is obtained through the Law of Propagation of Uncertainty as:

$$\boldsymbol{\Sigma}_{\boldsymbol{\epsilon}_{lk}} = \mathbf{E}_{lk}\boldsymbol{\Sigma}_{\mathbf{e}_{lk}}\mathbf{E}_{lk}^\mathsf{T} \quad (21)$$

where $\boldsymbol{\Sigma}_{\mathbf{e}_{lk}}$ is considered in the following, without loss of generality, diagonal and includes the uncertainty description of PMU measurements (here assumed decorrelated) or of averaged repeated measurements.

The covariance matrix of the prior $\boldsymbol{\Sigma}_{\mathbf{e}_{prior}}$ is the diagonal matrix including all the prior variances of the unknowns. If additional information on the correlations is available, it can be included too.

Finally, $\hat{\mathbf{x}}_{lk}$ is the estimated unknowns vector and is obtained through the solution of the WLS problem:

$$(\mathbf{H}_{lk,+}^\mathsf{T}\mathbf{W}_{lk,+}\mathbf{H}_{lk,+})\hat{\mathbf{x}}_{lk} = \left(\mathbf{H}_{lk,+}^\mathsf{T}\mathbf{W}_{lk,+}\right)\mathbf{b}_{lk,+} \quad (22)$$

D. Estimation Method for a Set of Branches

In Section II-C, the estimation method for a single branch, either a transmission line (i,j) or a voltage regulator branch (l,k), has been presented. The approach can be extended to

a set of branches or even to the entire network, considering a multiple instant problem like (18) for all the branches included in the portion of interest. The obtained systems can be merged so that all the voltage drop equations (6) and (15) and all the current-related equations (7) and (16) of all the involved branches are managed. A new overall system can thus be written as:

$$\mathbf{b}_+ = \begin{bmatrix} \mathbf{b}_{l_1 k_1} \\ \vdots \\ \mathbf{b}_{l_{N_{\mathrm{SVR}}} k_{N_{\mathrm{SVR}}}} \\ \mathbf{b}_{i_1 j_1} \\ \vdots \\ \mathbf{b}_{i_{N_{\mathrm{br}}} j_{N_{\mathrm{br}}}} \\ \mathbf{0}_{r_{tot} \times 1} \end{bmatrix} = \begin{bmatrix} \mathbf{H} \\ \mathbf{I}_{r_{tot}} \end{bmatrix} \mathbf{x} + \begin{bmatrix} \boldsymbol{\epsilon} \\ \mathbf{e}_{prior} \end{bmatrix} = \mathbf{H}_+ \mathbf{x} + \boldsymbol{\epsilon}_+$$

(23)

where N_{SVR} and N_{br} are the number of involved SVRs and lines, respectively, and $\mathbf{H}$ is the measurement matrix merging all the constraints given by all the considered equations. Vector $\mathbf{x}$ is the vector of all the unknowns and r_{tot} is its length. Considering different branches, systematic measurement errors can belong to multiple constraints, thus improving the measurement/constraint ratio and improving the estimation process. The solution of (23) can be obtained through WLS as in the single-branch approach and leads to a simultaneous estimation of the systematic deviations of all the involved measurements, the line parameters and the tap ratios, defining a three-phase formulation of the multi-branch approach used in [25].

III. TESTS AND RESULTS

The proposal has been validated by means of different types of tests carried out in a controlled environment in order to highlight properly the impact of different modelling on the estimation results. The tests have been performed on a three-phase version of the IEEE 14 bus test system (the equivalent diagram is shown in Fig. 2) simulated in MATLAB. The three-phase test system has been obtained by considering the data of the IEEE 14-bus test system as positive sequence parameters and then deriving negative and zero sequence values according to [15].

All the tests have been carried out simulating different realistic load conditions on the grid; each of them represents a case (see Section II), and repeated measurements are acquired for each case. To validate statistically the results, Monte Carlo (MC) simulations have been performed. In particular, $P = 10$ cases and $M = 10$ measurements for every case and each MC trial, and $N_{MC} = 10000$ trials have been considered. For each case, the reference values are obtained by means of a three phase powerflow, therefore the voltage and current measurements and actual tap ratio conditions are established. For each measurement instant and for each voltage and current measurement, systematic and random errors are then added to the reference values.

In the following, random errors are assumed to be mainly associated with PMUs and systematic errors are associated
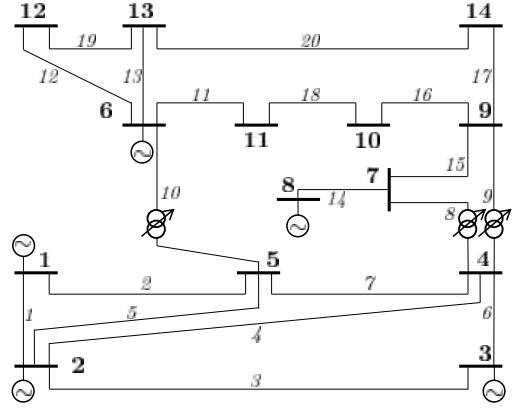

Fig. 2. Unifilar diagram of the IEEE 14-bus system.

with ITs. Thus, random contributions depend on the accuracy intervals given by PMU specifications, while systematic contributions basically depend on the accuracy class of ITs.

The setup is prepared according to the following assumptions:

1) As for the line parameters, maximum deviations of $R_{ij,pq}$, $X_{ij,pq}$ and $B_{\mathrm{sh},ij,pq}$ are equal to $\pm 10\,\%$.
2) As for the ITs (assumed of class 0.5 [30], [31]), a maximum error of $0.5\,\%$ for voltage and current ratios, a maximum CT phase-angle displacement of $0.9\,\mathrm{crad}$ ($10^{-2}\,\mathrm{rad}$) and a maximum VT phase-angle displacement of $0.6\,\mathrm{crad}$ are considered, while for $a_{lk,pq}$ the maximum deviation is $\pm 1\,\%$ [4].
3) As for the PMUs, a maximum amplitude error of $0.1\,\%$ and a maximum phase-angle error of $0.1\,\mathrm{crad}$ are used, corresponding to accurate but realistic values for real PMUs in steady-state conditions.
4) As for the operating conditions, a variability of $\pm 10\,\%$ with respect to nominal values for load/generator values (for both active and reactive powers) is considered among different load conditions. For each node, a maximum variability of $\pm 1\,\%$ of the nominal power has also been imposed among the phases, thus keeping the voltage asymmetry always compatible with that found by Italian TSO (see, e.g., [32] and [33]).
5) For every test, the errors and the deviations of all the parameters involved are extracted from uniform distributions.

The above assumptions (default scenario) are intended to describe in a meaningful way the variability in the network and the main uncertainty sources of the monitoring system.

To assess the performance of the proposal, the root mean square error (RMSE) is used:

$$\mathrm{RMSE} = \sqrt{\sum_{i=1}^{N_{MC}} \frac{(\hat{\nu} - \nu)^2}{N_{MC}}}$$

(24)

where $\hat{\ }$ indicates the estimated quantity. In (24) ν is a placeholder for each unknown of the state vector $\mathbf{x}$ or $\mathbf{x}_{hd}$ (with

$(h, d) = (i, j)$ or (l, k) indicating the generic branch). For phase p, ν can thus be equal to $\xi_{h,p}$, $\alpha_{h,p}$, $\xi_{d,p}$, $\alpha_{d,p}$, $\eta_{hd,p}$, $\psi_{hd,p}$, $\eta_{dh,p}$, $\psi_{dh,p}$, $\gamma_{hd,pq}$, $\beta_{hd,pq}$, $\rho_{hd,pq}$ and $\tau_{hd,pq}$, where $q \in \{a, b, c\}$ depending on the configurations and the models.

A. Single-Branch Approach

The first series of tests has been carried out using the single-branch approach to assess the performance of the proposed method on all three phase branches equipped with a step voltage regulator (branches $(4, 7)$, $(4, 9)$ and $(5, 6)$). Both SVR configurations presented in Section II-B have been adopted in different tests. For space reasons, in the following, the results are mainly reported for the closed delta configuration exploring all the estimated quantities, since it is much further from the single-phase model. All the RMSE results are compared with the corresponding standard deviations of the extracted errors or deviations in all N_{MC} trials. These standard deviations represent also the prior RMSE errors. In particular, standard deviation is $\Delta_\gamma/\sqrt{3} = \Delta_\beta/\sqrt{3} = \Delta_\rho/\sqrt{3} \simeq 5.77\,\%$ (Δ indicates the maximum deviation) for network parameters and $\Delta_\tau/\sqrt{3} \simeq 0.57\,\%$ for tap ratios, according to the assumed ranges. For systematic ratio error of voltage and current measurements the prior standard deviation is $\Delta_\xi/\sqrt{3} = \Delta_\eta/\sqrt{3} \simeq 0.29\,\%$, while it becomes $\Delta_\alpha/\sqrt{3} \simeq 0.35$ crad and $\Delta_\psi/\sqrt{3} \simeq 0.52$ crad for phase displacement error of voltage and current measurements, respectively. The estimation results of the proposal (referred to as "Tap estimation") are compared with those obtained with the method when tap ratios are considered as if they were perfectly known at run time ("No Tap estimation"). In the latter case, the deviations from assumed values, which actually occur, are neither included in the model nor estimated, since voltage regulation uncertainty is indeed neglected.

Table I reports the estimation results of phase displacement and voltage amplitude systematic errors for phase a (similar results can be found for the other system phases). When the tap changer is modelled, an RMSE reduction up to $50\,\%$ and $30\,\%$ for ratio errors and phase displacement errors, respectively, is achieved with respect to No Tap estimation. No Tap estimation indeed suffers from the lack of modeling and from the simplistic assumption of perfectly known tap ratios. Reductions of the same order are obtained for the current amplitude and phase displacement systematic errors. Similar results can also be obtained with wye configuration, with a $30\,\%$ RMSE reduction in the voltage ratio error. Nevertheless, as in [25], the advantages for phase displacement are instead negligible. It is important to highlight that, with Not Tap estimation the values of RMSE for ξ are beyond the prior ($0.29\,\%$), thus showing a critical degradation introduced by the estimator.

Table II shows the results for $\beta_{lk,pq}$, that is for the reactance estimation in SVR branches. Both estimation algorithms show RMSE values much lower than prior ($5.77\,\%$), but it is possible to observe a further reduction of estimation error (up to $37\,\%$ for branch 10) when the tap changer ratio is modelled and estimated.

Branch	Method	RMSE			
Index (l, k)		$\xi_{l,a}$ [%]	$\alpha_{l,a}$ [crad]	$\xi_{k,a}$ [%]	$\alpha_{k,a}$ [crad]
8 $(4, 7)$	Tap estimation	0.25	0.26	0.24	0.26
8 $(4, 7)$	No Tap estimation	0.48	0.35	0.48	0.36
9 $(4, 9)$	Tap estimation	0.24	0.26	0.24	0.26
9 $(4, 9)$	No Tap estimation	0.47	0.33	0.47	0.35
10 $(5, 6)$	Tap estimation	0.24	0.28	0.25	0.28
10 $(5, 6)$	No Tap estimation	0.44	0.31	0.43	0.33

Branch	Method	RMSE [%]		
Index (l, k)		$\beta_{lk,ab}$	$\beta_{lk,bc}$	$\beta_{lk,ac}$
8 $(4, 7)$	Tap estimation	2.76	2.76	2.72
8 $(4, 7)$	No Tap estimation	3.01	3.02	2.97
9 $(4, 9)$	Tap estimation	2.03	2.10	2.08
9 $(4, 9)$	No Tap estimation	2.75	2.81	2.81
10 $(5, 6)$	Tap estimation	2.31	2.33	2.33
10 $(5, 6)$	No Tap estimation	3.65	3.64	3.69

B. Multiple Branches Approach

Further analyses has been carried out with a multiple branches (multi-branch) approach. In particular, the entire three-phase network has been used in the estimation process thus including the constraints of all the branches. As a first result, Table III compares the RMSEs that can be obtained with multi-branch and single-branch approaches for tap changer ratio estimation (τ_{pq} parameters) considering closed delta connection. It is possible to see that the proposed method allows a remarkable reduction of the RMSE from prior value $0.57\,\%$ to less than $0.2\,\%$ with single-branch and less than $0.1\,\%$ with the multi-branch. With wye configuration, and the same loading conditions, the errors are higher, but single-branch approach still more than halves ($-54\,\%$) the RMSE with respect to prior and multi-branch solution, in turn, halves the estimation results obtained with the single-branch method, achieving reductions respect to prior errors of more than $77\,\%$.

Fig. 3 gives further insight into the estimation results, showing, for phase a as an example, the RMSEs for the estimation of the amplitude voltage systematic errors ($\xi_{h,a}$) as a function of the node index and obtained when the entire network is considered with the multi-branch approach. When the method is applied assuming the tap changer ratio as known, (blue squares) the estimation is jeopardized because the method suffers again from the lack of modelling. Indeed RMSEs are much higher than prior (black plus sign) and all the nodes are affected, even far away from the SVRs, thus preventing the

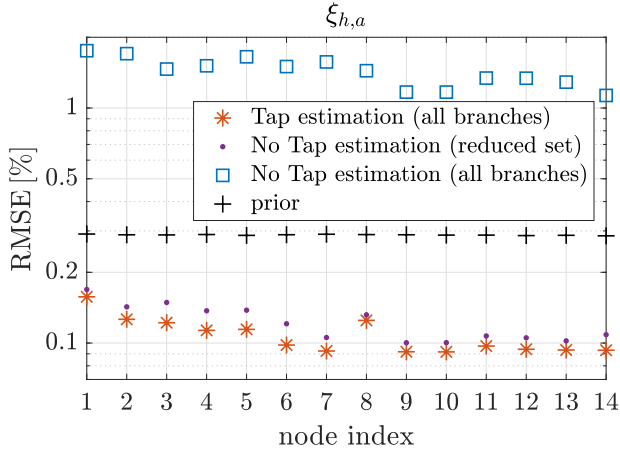| Branch Index (l,k)	Approach	RMSE [%]		
		$\tau_{lk,aa}$	$\tau_{lk,bb}$	$\tau_{lk,cc}$
8 $(4,7)$	Single-branch	0.18	0.18	0.18
8 $(4,7)$	Multi-branch	0.08	0.08	0.08
9 $(4,9)$	Single-branch	0.18	0.19	0.19
9 $(4,9)$	Multi-branch	0.08	0.08	0.08
10 $(5,6)$	Single-branch	0.19	0.19	0.19
10 $(5,6)$	Multi-branch	0.09	0.09	0.09

Fig. 3. Estimation of voltage amplitude systematic errors - results obtained with and without tap estimation.
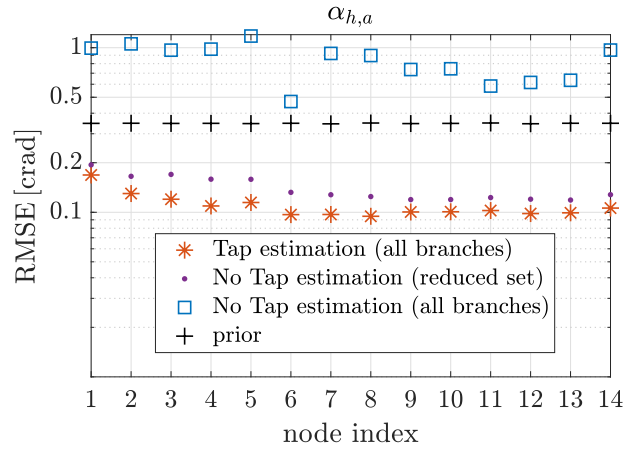

Fig. 4. Estimation of voltage phase-angle systematic errors - results obtained with and without tap estimation.
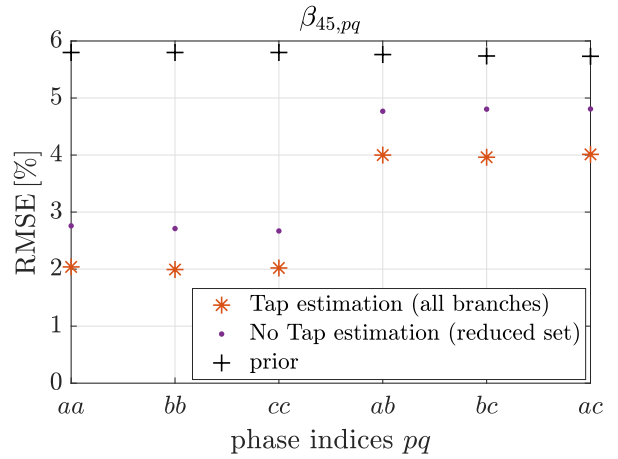
Fig. 5. RMSE results for the estimation of reactance parameters of branch $(4,5)$.

application of the method. Estimating the tap ratios and using the entire network (asterisks) brings a remarkable reduction of the errors with respect to the prior. This is confirmed also when looking at the estimation of systematic errors in voltage phase-angle displacement (Fig. 4, where the same methods, markers and colors as in Fig. 3 are used). It is also important to highlight that the No Tap estimation method, which does not consider deviations in the tap ratio, can be still applied to the the branches that do not include tap changers (purple dots). On this reduced set of branches, the proposed multi-branch three-phase method is much more accurate than prior, but the RMSEs are larger than the Tap estimation on all the nodes (up to about 24% for voltage magnitude and 47% for phase angle). The lowest RMSEs are thus obtained with the proposed method and the fully detailed model, resulting in an average improvement of about 68% with respect to the prior for phase angle errors. This type of results suggest also that a preliminary study on the network to monitor can help in designing the most appropriate estimation method to apply.

As an example, Fig. 5 reports the RMSE results for the parameters estimation of branch $(4,5)$, which is the branch next to the branches equipped with SVRs. In particular, the RMSE obtained for reactance deviations, with or without estimating the tap changer ratios, are shown (in the latter case the reduced set of branches is considered as above for a fair comparison). When the tap ratios are estimated, the uncertainty in the estimation of self reactances is lowered to almost one third of the prior uncertainty, while for mutual parameters RMSEs are reduced of about 30%, thus confirming the advantages of the proposed algorithm also in three-phase line estimation. A clear improvement is also brought by the complete model, leading to an RMSE reduction of more than 32% and 19% for self and mutual parameters, respectively, compared to the reduced set case. Similar results can be found also with SVRs in wye connection.

To investigate the impact of IT and PMU uncertainty on the estimation performance, tests have been performed considering different values for the IT class and the maximum PMU errors. IT with accuracy class 0.2 (0.2% as maximum ratio error and 0.3 crad as maximum phase displacement) is now considered. This implies prior standard deviations for ξ and α lower than in previous tests (0.12% and 0.17 crad, respectively). Table IV reports the RMSE results for both line parameters

and VT systematic errors, focusing on branch $(2,3)$. Similar results can be found also for other branches. As expected, the estimation accuracy degrades with higher uncertainties. In particular, since systematic errors are included in the model and estimated, the main impact is due to PMU errors, leading to an RMSE increase of more than $20\,\%$ for all the estimated line parameters when maximum PMU errors double.

TABLE IV
ESTIMATION PERFORMANCE UNDER DIFFERENT UNCERTAINTY
SCENARIOS

IT class	PMU accuracy $|\cdot|[\%], \angle[\text{crad}]$	RMSE							
		$\gamma_{23,aa}$ [%]	$\gamma_{23,ab}$ [%]	$\beta_{23,aa}$ [%]	$\beta_{23,ab}$ [%]	$\xi_{2,a}$ [%]	$\alpha_{2,a}$ [crad]	$\xi_{3,a}$ [%]	$\alpha_{3,a}$ [crad]
0.2	0.1, 0.1	2.11	2.81	1.39	2.81	0.07	0.08	0.06	0.07
	0.2, 0.2	2.63	3.37	1.67	3.47	0.08	0.11	0.07	0.09
0.5	0.1, 0.1	2.21	2.83	1.44	2.84	0.13	0.13	0.12	0.12
	0.2, 0.2	2.74	3.39	1.77	3.51	0.15	0.17	0.14	0.14

To investigate the impact on the estimation accuracy of the number of branches involved in the algorithm, tests have been performed considering the default scenario on a network size increasing progressively from a single branch to the entire network. Table V reports the RMSE results[2] for selected quantities focusing on branch $(2,3)$. As expected, the results improve with the size. The largest and most significant improvement for line-related parameters is achieved when two additional branches are included (error reduction up to about $26\,\%$ on an overall reduction with the whole network of about $34\,\%$), thus confirming the immediate advantage of a multi-branch approach. For systematic errors the effect is even more pronounced when the number of branches increases. For instance, the RMSE of $\alpha_{2,a}$ is almost halved on the entire network with respect to single-branch case. It is interesting to highlight that the improvements depend also on the network topology. Meshes, for instance, introduce additional constraints on the unknowns because each node is shared at least among two branches, thus helping the estimation process.

TABLE V
ESTIMATION PERFORMANCE ON INCREASING NETWORK PORTION -
BRANCH $(2,3)$

Network Portion	RMSE							
	$\gamma_{23,aa}$ [%]	$\gamma_{23,ab}$ [%]	$\beta_{23,aa}$ [%]	$\beta_{23,ab}$ [%]	$\xi_{2,a}$ [%]	$\alpha_{2,a}$ [crad]	$\xi_{3,a}$ [%]	$\alpha_{3,a}$ [crad]
Single-branch	3.24	4.06	2.20	4.29	0.22	0.26	0.22	0.26
3 branches	2.48	3.16	1.63	3.16	0.19	0.22	0.18	0.21
6 branches	2.43	3.09	1.56	3.12	0.14	0.17	0.15	0.18
All branches	2.21	2.83	1.44	2.84	0.13	0.13	0.12	0.12

Finally, even though an all-encompassing comparison with other methods from the literature is not possible, an example of the RMSE results (on branch $(2,3)$) achievable for line

[2]In Table V, "3 branches" corresponds to the set of branches with indexes 3, 4 and 6, while "6 branches" corresponds to branch indexes from 1 to 6.

parameters with different approaches using the same measurements is reported in Table VI. The proposed algorithm, which is used also in its single-branch version, is compared with two methods designed to estimate three-phase line parameters from PMU measurements. The first algorithm (Method A) is based on a two-step estimation of shunt admittance and impedance matrices of a branch [14], while the second algorithm (Method B) uses a robust estimator for the shunt and line admittance parameters starting from current equations at both ends [15]. The first method has been generalized to consider also non-transposed lines as the proposed one. These two methods rely on a significant level of unbalance to improve their accuracy. For this reason and to perform a fairer comparison with them, the maximum variations of the load power among the phases at a given node have been considered with two different levels (column 'Load Unb.'): $\pm 1\,\%$ and $\pm 5\,\%$ of the nominal power. In addition, following also the sensitivity study reported above, two classes of transducers and two PMU accuracy levels have been used. In the in Table VI, symbol '$>$' is used to indicate results far beyond (at least twice) the prior standard deviation of the parameters. It is clear that the proposed method shows lower RMSEs for all the parameters, whereas Methods A and B suffer low unbalance levels. In particular, the proposed method in its multi-branch configuration reaches the lowest RMSE and it clearly benefits from a higher unbalance level.

As a final comment, it is important to highlight that the three-phase formulation, besides allowing the estimation of three-phase parameters and the systematic errors that are intrinsically referred to the per-phase collected measurements, permits a better estimation also of positive sequence quantities when a realistic unbalance is present. To prove this, the positive sequence resistance and reactance of each line has been computed from the three-phase parameters estimated with the proposed method and directly with the single-phase version of [25]. The wye configuration has been used because an exact equivalence is possible with [25] in this case. The average estimation RMSEs across all the branches are reported in Table VII, where γ_+ and β_+ represent the relative deviations of positive sequence values from nominal ones for line resistance and reactance, respectively. The results confirm the advantages of the three-phase formulation when symmetry is no guaranteed in practice.

C. Experimental Results

To assess the performance of the proposed method with an even more realistic uncertainty description, additional tests have been performed using real measurement errors obtained through experimental laboratory characterization of commercial PMUs. As an example, Table VIII reports the RMSE results for system phase a and branches $(2,3)$, $(4,5)$ and $(9,14)$ when the experimental PMU errors are used. In particular, the amplitude and phase-angle errors recorded during the experiments have been added to the simulated quantities (after introducing IT systematic errors according to the assumed class 0.5) and the estimation has been performed with the proposed method (multi-branch). The RMSE results are similar

TABLE VI
COMPARISON AMONG DIFFERENT METHODS IN DIFFERENT UNCERTAINTY SCENARIOS - BRANCH (2, 3)

Method	ITs class	PMU accuracy $\|\cdot\|$[%], $\angle$[crad]	Load Unb. [%]	RMSE $\gamma_{23,aa}$ [%]	$\gamma_{23,ab}$ [%]	$\beta_{23,aa}$ [%]	$\beta_{23,ab}$ [%]
Proposed Method (All branches)	0.2	0.1, 0.1	1	2.11	2.81	1.39	2.81
			5	0.93	1.02	0.59	1.25
	0.5	0.1, 0.1	1	2.21	2.83	1.44	2.84
			5	1.08	1.07	0.67	1.33
		0.2, 0.2	1	2.74	3.39	1.77	3.51
			5	1.63	1.72	1.04	1.94
Proposed Method (Single branch)	0.2	0.1, 0.1	1	3.14	4.06	2.13	4.23
			5	1.47	1.64	0.97	2.07
	0.5	0.1, 0.1	1	3.22	4.07	2.19	4.29
			5	1.71	1.72	1.08	2.22
		0.2, 0.2	1	3.55	4.54	2.52	4.63
			5	2.56	2.81	1.72	3.35
Method A [14]	0.2	0.1, 0.1	1	>	>	>	>
			5	2.36	2.38	1.50	3.20
	0.5	0.1, 0.1	1	>	>	>	>
			5	3.30	3.42	2.09	4.62
		0.2, 0.2	1	>	>	>	>
			5	4.99	4.96	3.11	6.77
Method B [15]	0.2	0.1, 0.1	1	10.48	10.08	6.50	>
			5	2.14	2.22	1.40	2.92
	0.5	0.1, 0.1	1	>	>	8.40	>
			5	2.99	3.16	1.96	4.15
		0.2, 0.2	1	>	>	>	>
			5	4.45	4.55	2.86	6.05

TABLE VII
COMPARISON OF POSITIVE SEQUENCE PARAMETERS ESTIMATION WITH SINGLE-PHASE AND THREE-PHASE APPROACHES

Method	Average RMSE [%] γ_+	β_+
Single-phase	2.47	1.23
Three-phase	1.59	0.76

to those obtained with simulated PMU errors and even better since the used commercial PMUs have lower uncertainty than that assumed for previous tests. The RMSEs are much lower than prior standard deviations, thus confirming the validity of the presented approach in reducing the uncertainty of both network parameters and IT errors.

TABLE VIII
ESTIMATION PERFORMANCE WITH EXPERIMENTAL PMU ERRORS

Branch Index (i,j)	RMSE $\gamma_{ij,aa}$ [%]	$\gamma_{ij,ab}$ [%]	$\beta_{ij,aa}$ [%]	$\beta_{ij,ab}$ [%]	$\xi_{i,a}$ [%]	$\alpha_{i,a}$ [crad]	$\xi_{j,a}$ [%]	$\alpha_{j,a}$ [crad]
3 (2, 3)	1.81	2.36	1.10	2.29	0.11	0.11	0.11	0.11
7 (4, 5)	2.19	2.62	1.53	3.41	0.11	0.10	0.11	0.11
17 (9, 14)	1.62	1.91	1.39	3.27	0.09	0.10	0.09	0.10

IV. CONCLUSIONS

A novel method based on PMU measurements for the simultaneous estimation of systematic measurements errors, line parameters and tap changer ratios in a three-phase power systems has been presented in this paper. The method provides a framework to deal with different models of lines and regulators and can be adapted to different operator needs. It allows modelling the uncertainty introduced by the measurement chain together with the lack of knowledge in the network parameters. The estimation results obtained with the proposed method in a simulated environment under different uncertainty conditions and considering also experimental PMU errors show a remarkable improvement in the knowledge of the grid, thus fostering its extension to further models and instruments for a more accurate and complete monitoring of the power systems. The paper has also illustrated the risk of an incomplete description of the uncertainty, thus suggesting new research activities on measurement systems more aware of the available information quality.

APPENDIX

Equations A.25-A.28 (full width, top of next page) report the real and imaginary parts of the voltage drop and of the current balance equations for the wye connected SVR at branch (l, k) for all phases $p \in \{a, b, c\}$. Equations A.29-A.32 (full width, top of the last page) report the real and imaginary parts of the voltage drop and of the current balance equations for the closed delta connected SVR at branch (l, k) for phase a. Similar equations can be written for the other system phases.

REFERENCES

[1] M. Asprou, E. Kyriakides, and M. M. Albu, "Uncertainty Bounds of Transmission Line Parameters Estimated From Synchronized Measurements," *IEEE Trans. Instrum. Meas.*, vol. 68, no. 8, pp. 2808–2818, Aug. 2019.

[2] S. Vlahinic, D. Frankovic, M. Z. Durovic, and N. Stojkovic, "Measurement Uncertainty Evaluation of Transmission Line Parameters," *IEEE Trans. Instrum. Meas.*, vol. 70, pp. 1–7, Apr. 2021.

[3] C. A. Ferreira and R. B. Prada, "Improved model for tap-changing transformer," *IET Generation, Transmission & Distribution*, vol. 7, no. 11, pp. 1289–1295, Nov. 2013.

[4] *IEC/IEEE International Standard- Power transformers - Part 21: Standard requirements, terminology, and test code for step-voltage regulators*, IEC 60076-21:2018(E) IEEE Std C57.15-2017, 2018.

[5] A. Abur and A. Gómez Expósito, *Power system state estimation: theory and implementation*. New York, NY: Marcel Dekker, 2004.

[6] R. Yang, D. Zhang, Z. Li, K. Yang, S. Mo, and L. Li, "Mechanical fault diagnostics of power transformer on-load tap changers using dynamic time warping," *IEEE Trans. Instrum. Meas.*, vol. 68, no. 9, pp. 3119–3127, Sept. 2019.

[7] X. Liang, Y. Wang, and H. Gu, "A mechanical fault diagnosis model of on-load tap changer based on same-source heterogeneous data fusion," *IEEE Trans. Instrum. Meas.*, pp. 1–1, 2021.

[8] G. Korres, P. Katsikas, and G. Contaxis, "Transformer tap setting observability in state estimation," *IEEE Trans. Power Syst.*, vol. 19, no. 2, pp. 699–706, May 2004.

[9] A. Singhal, H. K. Rathour, P. Agarwal, K. V. S. Baba, and S. K. Soonee, "State estimation at all India level," in *2016 National Power Systems Conference (NPSC)*, Bhubaneswar, India, Dec. 2016, pp. 1–6.

[10] S. Corsi, M. Pozzi, C. Sabelli, and A. Serrani, "The coordinated automatic voltage control of the italian transmission grid-part i: reasons of the choice and overview of the consolidated hierarchical system," *IEEE Trans. Power Syst.*, vol. 19, no. 4, pp. 1723–1732, 2004.

$$V_{l,p}^r - V_{k,a}^r a_{lk,pp} + I_{lk,a}^x X_{lk,pp} a_{lk,pp}^2 \simeq V_{l,p}^r \left(\xi_{l,p}^{sys} + \xi_{l,p}^{rnd} \right) - V_{l,p}^x \left(\alpha_{l,p}^{sys} + \alpha_{l,p}^{rnd} \right) - V_{k,a}^r a_{lk,pp} \left(\xi_{k,a}^{sys} + \xi_{k,a}^{rnd} \right) +$$
$$+ V_{k,a}^x a_{lk,pp} \left(\alpha_{k,a}^{sys} + \alpha_{k,a}^{rnd} \right) + I_{lk,a}^x X_{lk,pp} a_{lk,pp}^2 \left(\eta_{lk,a}^{sys} + \eta_{lk,a}^{rnd} \right) + I_{lk,a}^x X_{lk,pp} a_{lk,pp}^2 \left(\psi_{lk,p}^{sys} + \psi_{lk,p}^{rnd} \right) +$$
$$- I_{lk,p}^x X_{lk,pp} a_{lk,pp}^2 \beta_{lk,pp} + \left(V_{k,a}^r a_{lk,pp} - 2 I_{lk,p}^x X_{lk,pp} a_{lk,pp}^2 \right) \tau_{lk,pp} \tag{A.25}$$

$$V_{l,p}^x - V_{k,a}^x a_{lk,pp} - I_{lk,p}^r X_{lk,pp} a_{lk,pp}^2 \simeq V_{l,p}^x \left(\xi_{l,p}^{sys} + \xi_{l,p}^{rnd} \right) + V_{l,p}^r \left(\alpha_{l,p}^{sys} + \alpha_{l,p}^{rnd} \right) - V_{k,a}^x a_{lk,pp} \left(\xi_{k,a}^{sys} + \xi_{k,a}^{rnd} \right) +$$
$$- V_{k,a}^r a_{lk,pp} \left(\alpha_{k,a}^{sys} + \alpha_{k,a}^{rnd} \right) - I_{lk,p}^r X_{lk,pp} a_{lk,pp}^2 \left(\eta_{lk,p}^{sys} + \eta_{lk,p}^{rnd} \right) + I_{lk,p}^x X_{lk,pp} a_{lk,pp}^2 \left(\psi_{lk,p}^{sys} + \psi_{lk,p}^{rnd} \right) +$$
$$+ I_{lk,p}^r X_{lk,pp} a_{lk,pp}^2 \beta_{lk,pp} + \left(V_{k,a}^x a_{lk,pp} + 2 I_{lk,p}^r X_{lk,pp} a_{lk,pp}^2 \right) \tau_{lk,pp} \tag{A.26}$$

$$I_{lk,p}^r a_{lk,pp} + I_{lk,p}^r \simeq I_{lk,p}^r a_{lk,pp} \left(\eta_{lk,p}^{sys} + \eta_{lk,p}^{rnd} \right) + I_{lk,p}^r \left(\eta_{lk,p}^{sys} + \eta_{lk,p}^{rnd} \right) - I_{lk,p}^x a_{lk,pp} \left(\psi_{lk,p}^{sys} + \psi_{lk,p}^{rnd} \right) +$$
$$- I_{lk,p}^x \left(\psi_{lk,p}^{sys} + \psi_{lk,p}^{rnd} \right) - I_{lk,p}^r a_{lk,pp} \tau_{lk,pp} \tag{A.27}$$

$$I_{lk,p}^x a_{lk,pp} + I_{lk,p}^x \simeq I_{lk,p}^x a_{lk,pp} \left(\eta_{lk,p}^{sys} + \eta_{lk,p}^{rnd} \right) + I_{lk,p}^x \left(\eta_{lk,p}^{sys} + \eta_{lk,p}^{rnd} \right) + I_{lk,p}^r a_{lk,pp} \left(\psi_{lk,p}^{sys} + \psi_{lk,p}^{rnd} \right) +$$
$$+ I_{lk,p}^r \left(\psi_{lk,p}^{sys} + \psi_{lk,p}^{rnd} \right) - I_{lk,p}^x a_{lk,pp} \tau_{lk,pp} \tag{A.28}$$

[11] S. Corsi, M. Pozzi, M. Sforna, and G. Dell'Olio, "The coordinated automatic voltage control of the italian transmission grid-part ii: control apparatuses and field performance of the consolidated hierarchical system," *IEEE Trans. Power Syst.*, vol. 19, no. 4, pp. 1733–1741, 2004.

[12] E. Mohns, P. Räther, and H. Badura, "An ac power standard for loss measurement systems for testing power transformers," *IEEE Trans. Instrum. Meas.*, vol. 66, no. 9, pp. 2225–2232, 2017.

[13] M. R. Rezaei, S. R. Hadian-amrei, and M. R. Miveh, "Online identification of power transformer and transmission line parameters using synchronized voltage and current phasors," *Electric Power Systems Research*, vol. 203, p. 107638, Feb. 2022.

[14] H. Goklani, G. Gajjar, and S. A. Soman, "Quantification of Minimum Unbalance Required for Accurate Estimation of Sequence Parameters of Transmission Line using PMU Data," in *2019 IEEE Power & Energy Society General Meeting (PESGM)*. Atlanta, GA, USA: IEEE, Aug. 2019, pp. 1–5.

[15] V. Milojević, S. Čalija, G. Rietveld, M. V. Ačanski, and D. Colangelo, "Utilization of pmu measurements for three-phase line parameter estimation in power systems," *IEEE Trans. Instrum. Meas.*, vol. 67, no. 10, pp. 2453–2462, Oct. 2018.

[16] R. Dutta, V. S. Patel, S. Chakrabarti, A. Sharma, R. K. Das, and S. Mondal, "Parameter estimation of distribution lines using scada measurements," *IEEE Trans. Instrum. Meas.*, vol. 70, pp. 1–11, 2021.

[17] W. Wang and N. Yu, "Estimate three-phase distribution line parameters with physics-informed graphical learning method," *IEEE Trans. Power Syst.*, pp. 1–1, 2021.

[18] R. C. Pires, L. Mili, and F. A. B. Lemos, "Constrained robust estimation of power system state variables and transformer tap positions under erroneous zero-injections," *IEEE Trans. Power Syst.*, vol. 29, no. 3, pp. 1144–1152, May 2014.

[19] M. Rezaei, S. S. Mortazavi, M. Razaz, and M. S. Ghazizadeh, "The statistical interval estimation of the mean and the hypothesis testing of population proportions for transformer tap position estimation," *Electric Power Systems Research*, vol. 164, pp. 212–219, Nov 2018.

[20] A. S. Dobakhshari, M. Abdolmaleki, V. Terzija, and S. Azizi, "Online Non-iterative Estimation of Transmission Line and Transformer Parameters Using SCADA Data," *IEEE Transactions on Power Systems*, vol. 36, no. 3, pp. 2632–2641, May 2021.

[21] C. Borda, A. Olarte, and H. Diaz, "PMU-based line and transformer parameter estimation," in *2009 IEEE/PES Power Systems Conference and Exposition*, Seattle, WA, USA, Mar. 2009, pp. 1–8.

[22] B. Vicol, "On-line overhead transmission line and transformer parameters identification based on PMU measurements," in *2014 Int. Conf. and Exposition on Electr. and Power Eng. (EPE)*, Iasi, Romania, Oct. 2014, pp. 1045–1050.

[23] S. G. Ghiocel *et al.*, "Phasor-measurement-based state estimation for synchrophasor data quality improvement and power transfer interface monitoring," *IEEE Trans. Power Syst.*, vol. 29, no. 2, pp. 881–888, March 2014.

[24] E. R. Fernandes *et al.*, "Application of a phasor-only state estimator to a large power system using real PMU data," *IEEE Trans. Power Syst.*, vol. 32, no. 1, pp. 411–420, Jan. 2017.

[25] P. A. Pegoraro, C. Sitzia, A. V. Solinas, and S. Sulis, "A pmu-based technique for the simultaneous estimation of systematic measurement errors, line parameters and tap changer ratio," in *2021 IEEE 11th International Workshop on Applied Measurements for Power Systems (AMPS)*, 2021, pp. 1–6.

[26] M. Bazrafshan, N. Gatsis, and H. Zhu, "Optimal power flow with step-voltage regulators in multi-phase distribution networks," *IEEE Trans. Power Syst.*, vol. 34, no. 6, pp. 4228–4239, May 2019.

[27] M. Bazrafshan and N. Gatsis, "Comprehensive modeling of three-phase distribution systems via the bus admittance matrix," *IEEE Trans. Power Syst.*, vol. 33, no. 2, pp. 2015–2029, March 2018.

[28] W. H. K. Kersting, *Distribution System Modeling and Analysis, 3rd ed.* Boca Raton, FL, USA: William H. Kersting, 2002.

[29] P. A. Pegoraro, K. Brady, P. Castello, C. Muscas, and A. von Meier, "Line Impedance Estimation Based on Synchrophasor Measurements for Power Distribution Systems," *IEEE Trans. Instrum. Meas.*, vol. 68, no. 4, pp. 1002–1013, Apr. 2019.

[30] *IEC 61869-2:2012. Instrument transformers - Part 2: Additional Requirements for Current Transformers*, IEC Int. Std., 2012.

[31] *IEC 61869-3:2012. Instrument transformers - Part 3: Additional Requirements for Inductive Voltage Transformers*, IEC Int. Std., 2012.

[32] Terna SpA, "Qualità del servizio di trasmissione - rapporto annuale per l'anno 2020 [Quality of service - Annual report for year 2020]," pp. 1–109, 2021, (in Italian). [Online]. Available: https://download.terna.it/terna/Rapporto%20Annuale%20Qualit%C3%A0%202020_8d942c0ff3f9277.pdf

[33] P. Castello, C. Muscas, P. A. Pegoraro, G. Guida, G. M. Giannuzzi, and P. Pau, "Interoperability of phasor measurement units under voltage unbalance conditions," in *2017 AEIT International Annual Conference*, 2017, pp. 1–6.

$$
\begin{aligned}
V_{l,a}^r - V_{k,b}^r - \left(V_{k,a}^r - V_{k,b}^r\right) a_{lk,ab} &+ \left[I_{lk,a}^x(2a_{lk,ab}^2 - 2a_{lk,ab} + 1) - I_{lk,c}^x a_{lk,ab}(a_{lk,ac} + 1) - I_{lk,b}^x a_{lk,bc}(a_{lk,ab} - 1)\right] X_{lk,ab}^0 \\
&\simeq V_{l,a}^r \left(\xi_{l,a}^{sys} + \xi_{l,a}^{rnd}\right) - V_{l,a}^x \left(\alpha_{l,a}^{sys} + \alpha_{l,a}^{rnd}\right) - V_{k,a}^r a_{lk,ab} \left(\xi_{k,a}^{sys} + \xi_{k,a}^{rnd}\right) + V_{k,a}^x a_{lk,ab} \left(\alpha_{k,a}^{sys} + \alpha_{k,a}^{rnd}\right) + \\
&+ V_{k,b}^r \left(a_{lk,ab} - 1\right) \left(\xi_{k,b}^{sys} + \xi_{k,b}^{rnd}\right) - V_{k,b}^x \left(a_{lk,ab} - 1\right) \left(\alpha_{k,b}^{sys} + \alpha_{k,b}^{rnd}\right) + \\
&+ I_{lk,a}^x X_{lk,ab}^0 \left(2a_{lk,ab}^2 - 2a_{lk,ab} + 1\right) \left(\eta_{lk,a}^{sys} + \eta_{lk,a}^{rnd}\right) + I_{lk,a}^r X_{lk,ab}^0 \left(2a_{lk,ab}^2 - 2a_{lk,ab} + 1\right) \left(\psi_{lk,a}^{sys} + \psi_{lk,a}^{rnd}\right) + \\
&- I_{lk,b}^x X_{lk,ab}^0 a_{lk,bc} \left(a_{lk,ab} - 1\right) \left(\eta_{lk,b}^{sys} + \eta_{lk,b}^{rnd}\right) - I_{lk,b}^r X_{lk,ab}^0 a_{lk,bc} \left(a_{lk,ab} - 1\right) \left(\psi_{lk,b}^{sys} + \psi_{lk,b}^{rnd}\right) + \\
&- I_{lk,c}^x X_{lk,ab}^0 a_{lk,ab} \left(a_{lk,ac} - 1\right) \left(\eta_{lk,c}^{sys} + \eta_{lk,c}^{rnd}\right) - I_{lk,c}^r X_{lk,ab}^0 a_{lk,ab} \left(a_{lk,ac} - 1\right) \left(\psi_{lk,c}^{sys} + \psi_{lk,c}^{rnd}\right) + \\
&+ \left[I_{lk,a}^x \left(a_{lk,ab}^2 + 2a_{lk,ab} - 1\right) + I_{lk,b}^x a_{lk,bc} \left(a_{lk,ab} - 1\right) + I_{lk,c}^x a_{lk,ab} \left(a_{lk,ac} - 1\right)\right] X_{lk,ab}^0 \beta_{lk,ab} + \\
&+ \left[V_{k,a}^r - V_{k,b}^r - 2I_{lk,a}^x X_{lk,ab}^0 (2a_{lk,ab} - 1) + I_{lk,b}^x X_{lk,ab}^0 a_{lk,bc} + I_{lk,c}^x X_{lk,ab}^0 (a_{lk,ac} - 1)\right] a_{lk,ab} \tau_{lk,ab} + \\
&+ I_{lk,b}^x X_{lk,ab}^0 a_{lk,bc} \left(a_{lk,ab} - 1\right) \tau_{lk,bc} + I_{lk,c}^x X_{lk,ab}^0 a_{lk,ab} a_{lk,ac} \tau_{lk,ac}
\end{aligned}
\tag{A.29}
$$

$$
\begin{aligned}
V_{l,a}^x - V_{k,b}^x - \left(V_{k,a}^x a_{lk,ab} - V_{k,b}^x\right) &- \left[I_{lk,a}^r \left(2a_{lk,ab}^2 - 2a_{lk,ab} + 1\right) + I_{lk,b}^r a_{lk,bc} \left(a_{lk,ab} - 1\right) + I_{lk,c}^r a_{lk,ab} \left(a_{lk,ac} - 1\right)\right] X_{lk,ab}^0 \\
&\simeq V_{l,a}^x \left(\xi_{l,a}^{sys} + \xi_{l,a}^{rnd}\right) + V_{l,a}^r \left(\alpha_{l,a}^{sys} + \alpha_{l,a}^{rnd}\right) - V_{k,a}^x a_{lk,ab} \left(\xi_{k,a}^{sys} + \xi_{k,a}^{rnd}\right) - V_{k,a}^r a_{lk,ab} \left(\alpha_{k,a}^{sys} + \alpha_{k,a}^{rnd}\right) + \\
&+ V_{k,b}^x \left(a_{lk,ab} - 1\right) \left(\xi_{k,b}^{sys} + \xi_{k,b}^{rnd}\right) + V_{k,b}^r \left(a_{lk,ab} - 1\right) \left(\alpha_{k,b}^{sys} + \alpha_{k,b}^{rnd}\right) + \\
&- I_{lk,a}^r X_{lk,ab}^0 \left(2a_{lk,ab}^2 - 2a_{lk,ab} + 1\right) \left(\eta_{lk,a}^{sys} + \eta_{lk,a}^{rnd}\right) + I_{lk,a}^x X_{lk,ab}^0 \left(2a_{lk,ab}^2 - 2a_{lk,ab} + 1\right) \left(\psi_{lk,a}^{sys} + \psi_{lk,a}^{rnd}\right) + \\
&+ I_{lk,b}^r X_{lk,ab}^0 a_{lk,bc} \left(a_{lk,ab} - 1\right) \left(\eta_{lk,b}^{sys} + \eta_{lk,b}^{rnd}\right) - I_{lk,b}^x X_{lk,ab}^0 a_{lk,bc} \left(a_{lk,ab} - 1\right) \left(\psi_{lk,b}^{sys} + \psi_{lk,b}^{rnd}\right) + \\
&+ I_{lk,c}^r X_{lk,ab}^0 a_{lk,ab} \left(a_{lk,ac} - 1\right) \left(\eta_{lk,c}^{sys} + \eta_{lk,c}^{rnd}\right) - I_{lk,c}^x X_{lk,ab}^0 a_{lk,ab} \left(a_{lk,ac} - 1\right) \left(\psi_{lk,c}^{sys} + \psi_{lk,c}^{rnd}\right) + \\
&+ \left[I_{lk,a}^r \left(2a_{lk,ab}^2 - 2a_{lk,ab} + 1\right) - I_{lk,b}^r a_{lk,bc} \left(a_{lk,ab} - 1\right) + I_{lk,c}^r a_{lk,ab} a_{lk,ac}\right] X_{lk,ab}^0 \beta_{lk,ab} + \\
&+ \left[V_{k,a}^x - V_{k,b}^x + 2I_{lk,a}^r X_{lk,ab} \left(2a_{lk,ab} - 1\right) - I_{lk,b}^r X_{lk,ab} a_{lk,bc} - I_{lk,c}^r X_{lk,ab} \left(a_{lk,ac} - 1\right)\right] a_{lk,ab} \tau_{lk,ab} + \\
&- I_{lk,b}^r X_{lk,ab} a_{lk,bc} \left(a_{lk,ab} - 1\right) \tau_{lk,bc} - I_{lk,c}^r X_{lk,ab} a_{lk,ab} a_{lk,ac} \tau_{lk,ac}
\end{aligned}
\tag{A.30}
$$

$$
\begin{aligned}
I_{lk,a}^r(a_{lk,ab} + 1) - I_{lk,c}^r(a_{lk,ac} - 1) &\simeq -I_{lk,a}^r a_{lk,ab} \tau_{lk,ab} + I_{lk,c}^r a_{lk,ac} \tau_{lk,ac} + \\
&+ I_{lk,a}^r a_{lk,ab} \left(\eta_{lk,a}^{sys} + \eta_{lk,a}^{rnd}\right) - I_{lk,c}^r \left(a_{lk,ac} - 1\right) \left(\eta_{lk,c}^{sys} + \eta_{lk,c}^{rnd}\right) + I_{kl,a}^r \left(\eta_{kl,a}^{sys} + \eta_{kl,a}^{rnd}\right) + \\
&- I_{lk,a}^x a_{lk,ab} \left(\psi_{lk,a}^{sys} + \psi_{lk,a}^{rnd}\right) + I_{lk,c}^x \left(a_{lk,ac} - 1\right) \left(\psi_{lk,c}^{sys} + \psi_{lk,c}^{rnd}\right) - I_{kl,a}^x \left(\psi_{kl,a}^{sys} + \psi_{kl,a}^{rnd}\right)
\end{aligned}
\tag{A.31}
$$

$$
\begin{aligned}
I_{lk,a}^x(a_{lk,ab} + 1) - I_{lk,c}^x(a_{lk,ac} - 1) &\simeq -I_{lk,a}^x a_{lk,ab} \tau_{lk,ab} + I_{lk,c}^x a_{lk,ac} \tau_{lk,ac} + \\
&+ I_{lk,a}^x a_{lk,ab} \left(\eta_{lk,a}^{sys} + \eta_{lk,a}^{rnd}\right) - I_{lk,c}^x \left(a_{lk,ac} - 1\right) \left(\eta_{lk,c}^{sys} + \eta_{lk,c}^{rnd}\right) + I_{kl,a}^x \left(\eta_{kl,a}^{sys} + \eta_{kl,a}^{rnd}\right) + \\
&+ I_{lk,a}^r a_{lk,ab} \left(\psi_{lk,a}^{sys} + \psi_{lk,a}^{rnd}\right) - I_{lk,c}^r \left(a_{lk,ac} - 1\right) \left(\psi_{lk,c}^{sys} + \psi_{lk,c}^{rnd}\right) + I_{kl,a}^r \left(\psi_{kl,a}^{sys} + \psi_{kl,a}^{rnd}\right)
\end{aligned}
\tag{A.32}
$$

Paolo Attilio Pegoraro (Senior Member, IEEE) received the M.S. (*summa cum laude*) degree in telecommunication engineering and the Ph.D. degree in electronic and telecommunication engineering from the University of Padova, Padua, Italy, in 2001 and 2005, respectively.

From 2015 to 2018 he was an Assistant Professor with the Department of Electrical and Electronic Engineering, University of Cagliari, Cagliari, Italy, where he is currently Associate Professor. He has authored or coauthored over 120 scientific papers. His current research interests include the development of new measurement techniques for modern power networks, with attention to synchronized measurements and state estimation.

Dr. Pegoraro is a member of IEEE IMS TC 39 (Measurements in Power Systems) and of IEC TC 38/WG 47. He is an Associate Editor of the IEEE Transactions on Instrumentation and Measurement.

Carlo Sitzia (Student Member, IEEE) received the M.S. degree (cum laude) in electrical engineering from the University of Cagliari, Cagliari, Italy, in 2020, where he is currently pursuing the Ph.D. degree with the Electrical and Electronic Measurements Group, Department of Electrical and Electronic Engineering.

His research activities focus on parameter estimation for modern power networks, phasor measurements, and instrument transformers.

Antonio Vincenzo Solinas (Graduate Student Member, IEEE) received the M.S. degree in Electronic Engineering from University of Cagliari, Italy, in 2000, where he is currently pursuing the Ph.D. degree with the Electrical and Electronic Measurements Group, Department of Electrical and Electronic Engineering.

Since 2000, he worked as an R&D manager on audio and video acquisition, compression and transmission over IP. His main research interests include the optimization techniques for estimation and monitoring in power systems.

Sara Sulis (Senior Member, IEEE) received the M.S. degree in electrical engineering and the Ph.D. degree in industrial engineering from the University of Cagliari, Cagliari, Italy, in 2002 and 2006, respectively.

She is currently an Associate Professor of electrical and electronic measurements with the University of Cagliari. She has authored or coauthored more than 100 scientific articles. Her current research interests include distributed measurement systems designed to perform state estimation and harmonic sources estimation of distribution networks.

Dr. Sulis is a member of the Instrumentation and Measurement Society, the IEEE TC 39 "Measurements in Power Systems," and the CENELEC TC 38 "Instrument Transformers." She is an Associate Editor of the IEEE Transactions on Instrumentation and Measurement.